Proceedings of ASME Turbo Expo 2019
Turbo Expo 2019
June 17-21, 2019, Phoenix AZ, USA

GT2019-91379

DYNAMIC RESPONSE OF ACOUSTICALLY FORCED TURBULENT PREMIXED BIOGAS FLAMES

Oluwaseun Ajetunmobi
Department of Mechanical Engineering
University College London
London WC1E 7JE, UK
oluwaseun.ajetunmobi.16@ucl.ac.uk

Midhat Talibi*
Department of Mechanical Engineering
University College London
London WC1E 7JE, UK
m.talibi@ucl.ac.uk

Ramanarayanan Balachandran
Department of Mechanical Engineering
University College London
London WC1E 7JE, UK
r.balachandran@ucl.ac.uk

ABSTRACT

Increasing demand for energy and the need for diversification of fuels used in gas turbine power generation is continuing to drive forward the development of fuel-flexible combustion systems, with particular focus on biomass derived sustainable fuels. The technical challenges arising from burning sustainable fuels are largely associated with the change in the chemical, thermal and transport properties of these fuels due to the variation of the constituents and their impact on the performance of the combustor including emissions, static and dynamic stabilities. There is a lack of detailed understanding on the effect of fuel composition on the flame sensitivity to acoustic and flow perturbations.

This paper describes an experimental study investigating the acoustic flame response of simulated biogas (methane/carbon dioxide/air mixtures) turbulent premixed flames. The effect of variation in carbondioxide, CO_2, content on the flame response was quantified. Special emphasis was placed on understanding the dependence of this flame response on the amplitude of the acoustic forcing. The flame was subjected to strong velocity perturbations using loud speakers.

It was observed that the addition of CO_2 had considerable influence on the magnitude of heat release response. The magnitude and the phase of flame describing function indicated that the mechanism of saturation in these flames for all conditions tested were the same. The difference in magnitude could been attributed to dilution effect and hence further investigation were carried out with N_2 and Ar to clarify the role of CO_2. The results indicate that the thermal capacity of the diluent gases could be playing a significant role in nonlinear flame dynamics.

NOMENCLATURE

Q	flowrate
ϕ	equivalence ratio
f	frequency
U	bulk velocity
A	normalised amplitude
φ/π	normalised phase

1 INTRODUCTION

The requirement for substantial reduction in regulated hazardous emissions and the need for decarbonisation are two major challenges that directly impact the development and utilisation of gas turbines in power generation and transport sector. Particular focus is placed on reduction in NOx and particulate emissions, and addressed by governments via stringent environmental policies, as these emissions have been proven to contribute to various health problems. As a consequence, lean burn technologies are commonly adopted to reduced these emissions, and for improving efficiency. Utilisation of biogas and biomethane offers important opportunities for decarbonisation without substantial changes in infrastructure or operational strategies [1–3]. Thus, the combination of the right choice of fuel and combustion strategy (i.e. mode of combustion) could help gas turbine manufacturers meeting the above mentioned challenges.

*Corresponding author

Lean burn combustion systems used to achieve high fuel efficiency and lower pollutant emissions, for power generation and propulsion, are known to be susceptible to thermoacoustic instabilities. Lean burn operation allows substantial reduction in flame temperature and in particle emissions, however these operating conditions are prone to undesired complex resonant feedback interaction between the heat release rate variations in flames and the different acoustic modes which can cause pressure and flow oscillations. These oscillations may lead to excessive vibrations which can eventually result in complete breakdown of the power plant/system. There are number of mechanisms that could trigger interactions between acoustic oscillations and heat release in combustion systems. The following mechanisms have been identified and studied in literature: flame-acoustic wave interactions, flame vortex interactions, equivalence ratio oscillations and flame-wall interactions [4–6].

Gas turbines manufactures are keen to develop combustion systems that are fuel-flexible [7–9]. The major attraction for the use of fuel-flexible systems is their ability in utilising fuels from varied supply sources. Biogas and biomethane are among the various sustainable fuels that have potential for utilisation in natural gas burning combustion systems with minimum modification. Biogas is generally produced from the anaerobic digestion of biomass or organic waste, such as industrial waste gases containing hydrogen and carbon-dioxide. Anaerobic digestion is a biological process that happens when bacteria breaks down organic matter in environment with little or no oxygen. Typical biogas consists of N_2, CO_2, CH_4 and C_2H_6, however, the proportion could vary [10]. Biomethane is upgraded biogas with a higher percentage of methane. The variation in composition of the fuel plays an important role in pollutant emissions and may also affect the flame stability.

The role of carbondioxide (CO_2) in biogas flames was investigated numerically by Ju et al. [11]. The radiation and reabsorption effect of CO_2 had a significant effect on flame speed and the flammability limits, and the influence was highest at lean conditions particularly close to extinction. It is to be expected that the addition of CO_2 on the combustion is effected through the variation of both transport and thermal properties of the mixture. Furthermore, CO_2 could actively participate in the combustion kinetics [12–14]. It was shown experimentally by Shy et al. [15] that during combustion of methane/carbondioxide/air mixtures, the radiation losses due to CO_2 have a strong influence on the combustion intensity. Therefore the impact on flame by the diluents in the fuel can be summarised in three ways, through changes in (1) mixture specific heat and adiabatic flame temperature, (2) chemical kinematic rates, and (3) radiative heat transfer. All the above can influence the heat release from flames. This work will aim to study the effect of CO_2 content in methane flames on acoustic response, and the related role of adiabatic flame temperature and the specific heat capacities. Furthermore, there is lack of information on the non-linear flame response of biogas flames and saturation mechanisms that are relevant to thermo-acoustic instabilities in practical systems.

The specific objective of this paper is to compare the acoustic flame response of methane (CH_4) flames to that of simulated biogas (CH_4 + CO_2) flames of varying CO_2 proportions. Additionally, other diluent gases such as nitrogen (N_2) and argon (Ar) were studied, to clarify the role of diluents on the nonlinear flame response. The paper is structured as follows: the description of the combustor, measurement methods and data reduction procedures are provided, followed by results and discussion regarding the effect of CO_2, N_2 and Ar addition and conclusions.

2 EXPERIMENTAL METHODS

This section describes the burner, measurement methods and data processing procedures.

2.1 Bluff-body Combustor

The tests were conducted on a bluff-body stabilised combustor, the design of which is based on Ref. [16], and a schematic is shown in Fig. 1(a). The plenum has an internal diameter of 100 mm and and an overall length of 300 mm, including the divergent and convergent sections at the inlet and exit of the plenum prevented flow separation. The honeycomb mesh placed at the base of the plenum streamlined the flow. The duct leading on from the plenum enables acoustic pressure measurements for the two-microphone method, and is of length 400 mm and internal diameter 35 mm. The bluff body used in this combustor was conical in shape, with diameter 30 mm and blockage ratio $\approx$75%. An enclosure of square cross-section (100 mm x 100 mm x 100 mm) made of UV quartz prevented air entrainment from the surroundings. The flow was acoustically excited using two loudspeakers. A sinusoidal signal from National Instruments signal generator was amplified and supplied to the loud speakers. The peak-to-peak voltage of the forcing signal was varied to increase the forcing amplitude. Two frequencies, 260 Hz and 345 Hz, which provided high acoustic forcing amplitude were used to study the amplitude dependence of the acoustic flame response.

2.2 Measurement Methods

Flow rate measurements: Compressed air was delivered from a central facility, while the fuel (methane) and diluent gases were supplied from compressed gas cylinders. The flow rates of air, methane and diluent gases were controlled by high precision needle valve and the mass flow rates were measured using Bronkhorst MASS-VIEW high precision mass flow meters. The flow ranges of air, methane, CO_2, N_2 and Ar flow meters were 2-200 slpm, 0.2-20 slpm, 0.05-10 slpm, 0.05-10 slpm and 0.08-5 slpm, in that order. The accuracy of these mass flow meters was $\pm$ 1.5% Full Scale Division (FSD).

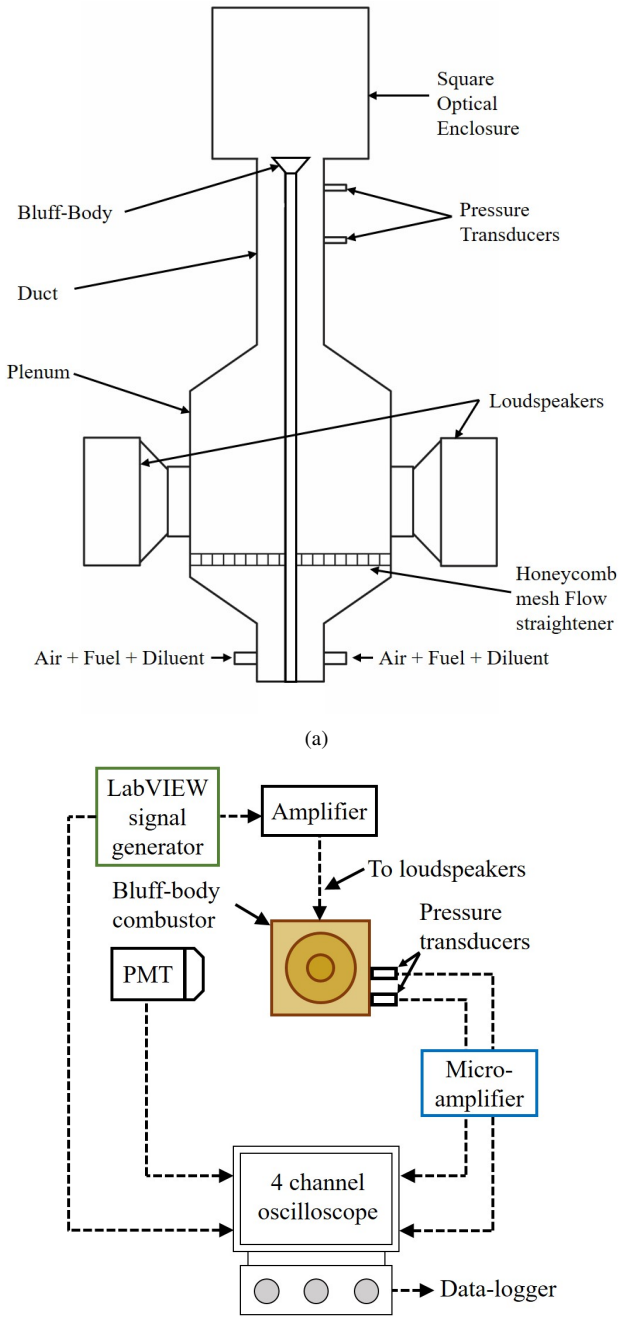

FIGURE 1. SCHEMATIC OF (a) THE COMBUSTOR, (b) THE EXPERIMENTAL ARRANGEMENT

Acoustic pressure measurements: Two high-sensitivity KuLite pressure transducers (Model XCS-093), positioned at locations 93 mm and 380 mm upstream of the bluff body plane, were used to record pressure fluctuations in the flow passage. The sensitivity of the transducers were 4.2857×10^{-3} mV/Pa. The signal from the transducers were amplified using two channel Flyde Micro Analogue amplifiers. The amplified signal is digitised and saved using a digital oscilloscope.

Heat release measurements: Heat release from the flames were quantified from OH* chemiluminescence emission. The use of OH* chemiluminescence and the limitations related estimating heat release modulation can be found in [16–18]. The OH* chemiluminescence emission were measured using an UV-sensitive fast response side-on Photomultiplier tube, PMT (Hamamatsu R3788). The emissions from the entire combustion zone was collected using a plano-convex lens. An interference filter of 10 nm bandwidth centered at 307 nm was used to isolate OH* chemiluminescence emission. The signal was recorded simultaneously with acoustic pressure and the reference forcing signal (input to the amplifier for the speakers) using the digital oscilloscope.

Data acquisition and recording: A four channel digital oscilloscope Tektronix DPO3014 was used to simultaneously record the reference signal, acoustic pressures from two transducers and the chemiluminescence from the PMT. The signals were acquried at a sampling rate of 50 kHz and the time series lasting 2 seconds were recorded and stored for post-processing.

2.3 Determination of Acoustic Flame Response

Typical time-trace of the forcing signal (that serves as input to the amplifier, referred as Ref. Signal), OH* chemiluminescence, $OH^*(t)$, and pressure, $p(t)$, captured using oscilloscope is presented in Fig. 2. The forcing frequency f for the data presented in Fig. 2 is 260 Hz. The time t has been normalised using time period t_p. It is clear from the figure that the modulation of heat release and pressure are sinusoidal for the case presented. Fast Fourier Transform (FFT) technique was used to analyse the $OH^*(t)$, $p(t)$ and the time-traces of Ref. Signal. The magnitude of the power spectrum for each of these parameters normalised with their respective maximum value is presented in Fig. 3. It can be seen from the figure that the dominant frequency observed from both the pressure and OH* power spectra corresponded to the forcing frequency. The complex amplitude of the quantity at the forcing frequency, $OH^{*\prime}(f)$ is normalised using time mean $\langle OH^* \rangle$ and this normalised value $OH^{*\prime}(f)/\langle OH^* \rangle$ can be used as an estimate for heat release fluctuation, $q'(f)/\langle q \rangle$. In this paper, $OH^{*\prime}(f)/\langle OH^* \rangle$ will be used to indicate the normalised heat release fluctuation. The amplitude of forcing $u'(f)/\langle U \rangle$ was estimated using velocity fluctuations, $u'(f)$, from two microphone method and the bulk mean velocity, $\langle U \rangle$. Details of the two microphone method can be found in Refs. [16, 19]. The flame describing function, FDF, (also known as the non-linear flame transfer function, $NFTF$) was determined from the ratio of the heat release fluctuations and the velocity

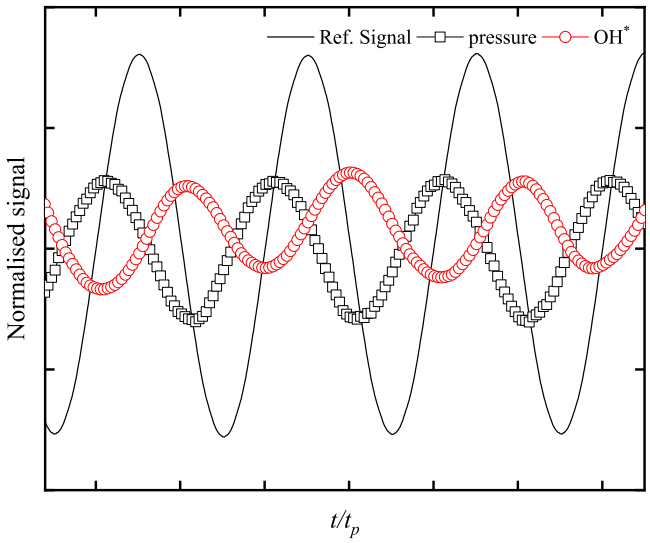

FIGURE 2. TYPICAL TIME-SERIES DATA FROM OH* USING PMT, ACOUSTIC PRESSURE MEASUREMENT USING TRANSDUCERS AND THE REFERENCE SIGNAL SUPPLIED TO THE AMPLIFIER FOR f=260 Hz : Q_{air} = 130 lpm, Q_f = 11 lpm, i.e ϕ=0.95.

perturbations, $FDF(f,u'(f)/\langle U\rangle) = (q'(f)/\langle q\rangle)/(u'(f)/\langle U\rangle)$ $=(OH^{*\prime}(f)/\langle OH^{*}\rangle)/(u'(f)/\langle U\rangle)$. Further details regarding the definition and importance of FDF can be found in Refs. [16, 20].

The frequency resolution relevant to FFT calculated from sampling rate and the number of sample recorded for this study is 0.5 Hz.

3 RESULTS AND DISCUSSION

3.1 Unforced and Forced Methane/Air Flame

The flowrates of air, Q_{air}, and methane, Q_f, for the reference case were chosen based on the following considerations: 1) to achieve high Reynolds number for turbulent combustion 2) to operate at high bulk velocity to avoid flame flashback and 3) to have a compact flame to minimise entrainment. The air and methane CH_4 flowrates identified were Q_{air}=181 lpm and Q_f=18 lpm i.e ϕ=0.95, $\langle U\rangle$=13 m/s respectively. The appearance and shape of the flame was consistent with other previous work [10, 16, 21]. The power spectra of OH^* and pressure signal for the unforced flame (see Fig. 4) indicate typical turbulent combustion behaviour, i.e broad band noise with some small feedback interference. When compared to the magnitude of the signal of forced flames (in Fig. 3) , the magnitude of this broadband noise is at negligible levels. The power spectra of the pressure signal presented in fig. 4 is typical of a turbulent flow in a pipe. The observations related to the general appearance of the flames (not presented here) indicated the following: i) unforced condition - blue flame stabilised on the bluff-body which

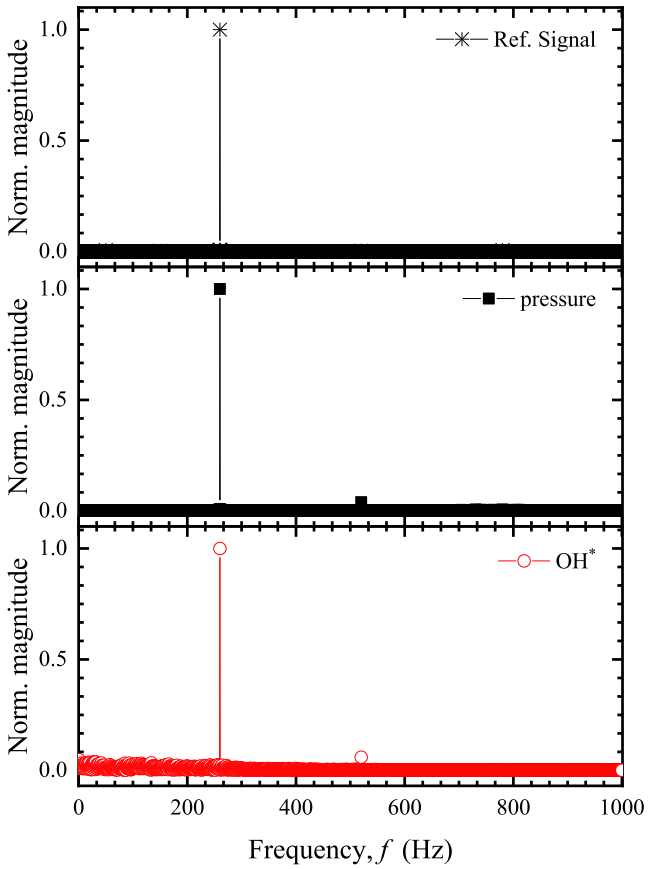

FIGURE 3. MAGNITUDE OF POWER SPECTRAL DENSITY NORMALISED BY THE RESPECTIVE MAXIMUM VALUES FOR DATA PRESENTED IN FIG. 2 : Q_{air} = 130 lpm, Q_f = 11 lpm, i.e ϕ=0.95.

extended to entire combustion length and ii) forced condition - blue flame stabilised on the bluff-body with a reduction in overall flame height. This is consistent with observation from other work [10, 21]. The observation related to flame height reduction is attributed to strong flame-vortex interaction.

The amplitude dependence of heat release response for the reference flame (ϕ=0.95, $\langle U\rangle$=13 m/s, referred as 0% Diluent) at a forcing frequency of $f = 260$ Hz is presented in Fig. 5. It can be seen from the figure that with an increase in the magnitude of forcing amplitude, initially there was a linear increase in normalised heat release modulation, followed by drastic reduction (non-linear variation). This leveling off of the response is called flame response'saturation'. The saturation in heat release response could be a consequence of strong flame-vortex interaction, similar to observations in Refs [10, 16]. The amplitude dependence of the heat release response at $f = 345$ Hz presented in Fig. 6 exhibited a similar trend. However, the amplitude at which the saturation occurred decreased with increased frequency (i.e.,

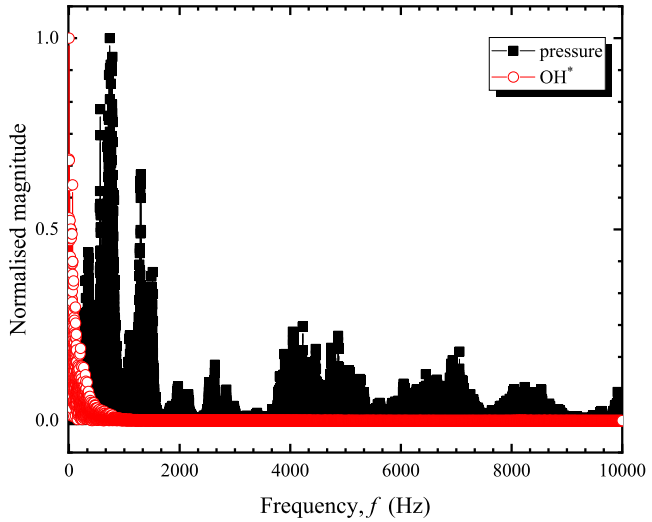

FIGURE 4. MAGNITUDE OF POWER SPECTRAL DENSITY NORMALISED BY THE RESPECTIVE MAXIMUM VALUES FOR THE REFERENCE CASE WITH NO ACOUSTIC FORCING: Q_{air} = 130 lpm, Q_f = 11 lpm, i.e ϕ=0.95.

the values of A at which saturation occurred for forcing frequencies, $f = 260$ Hz and 345 Hz were ≈ 0.38 and 0.28 respectively). The amplitude dependence of the magnitude and the phase (φ normalised by π of the flame describing function for frequencies 260 Hz and 345 Hz are presented in Figs. 7 and 8 respectively. The magnitudes of the flame describing function, $|FDF|$, confirms the observations made from Figs. 5 and 6. The normalised phase (φ/π) for 260 Hz and 345 Hz forcing exhibited slight increase with increasing amplitude that could be associated with appearance of vortices in flame [16]. For $f = 260$, at $A \approx 0.58$ the phase showed sudden reduction, while the magnitude reduction is gradual. This additional variation in flame response requires further investigation. It has to be noted that the magnitude of flame response at 260 Hz is about three-fold higher than at 345 Hz.

3.2 Effect of CO_2 Addition on Flame Response

In order to study the effect of carbondioxide, CO_2, content on the nonlinear response of the flames, CO_2 gas was added to the reference flame. The flowrate of CO_2 was varied in increments of 10% of fuel volume flow rate, upto 40 % (i.e., 10%, 20%, 30%, and 40%). The flame response for forcing frequencies of 260 Hz and 345 Hz are presented in Figs. 5- 8 .

It is clearly evident from Figs. 5 and 7 that there was a systematic decrease in heat release rate magnitudes (and the values of $|FDF|$) with increasing CO_2 addition. However, magnitude of flame response (normalised heat release fluctuation and $|FDF|$), when forced at $f = 345$ Hz, was not systematic; after 10% CO_2 addition the flame response seems to have a weak dependence on the percentage addition of CO_2. The saturation magnitude for forcing frequency $f = 260$ Hz for all CO_2 additions, except for 40% case, was around $A \approx 0.38$ (see Figs. 5 and 7). It can been seen clearly that the $|FDF|$ trend for 40 % CO_2 addition at $f = 260$ Hz had a significantly different amplitude dependency when compared to that of the other cases, including the reference case (0% Diluent). The $|FDF|$ at $f = 260$ Hz, for all cases, except 40% CO_2 addition, was relatively constant until $A \approx 0.38$, and then reduced beyond that value. However, $|FDF|$ had a decreasing trend for the 40 % addition of CO_2 at $f = 260$ Hz. When forcing at $f = 345$ Hz, the $|FDF|$ values and the trends were more or less the same for the reference case and 10% CO_2 addition, with slightly increasing values initially followed by a reduction. However, the rest of the cases (i.e, % additions of 20,30 and 40) exhibited decreasing trend, very similar to that of the 40% CO_2 addition at 260 Hz. The amplitude dependence of phase of FDF are similar for all CO_2 additions presented, for a fixed forcing frequency condition. The gradual variation in phase can be associated to kinematics of the flame, particularly to the flame-vortex rollup and subsequent dynamics [16].The observed trends in the effect of CO_2 on the magnitude of the heat release response can be attributed to the combined effect of reduction in flame temperature due to dilution effect and chemical interaction. The reduction in flame temperatures is expected to result in decreased recirculation temperatures and also cause an overall reduction in the mean heat release. The observed differences in FDF with CO_2 addition can be attributed to the flame response to vorticity. This is because at lower forcing amplitudes no apparent change can be seen, it is only at the higher amplitudes (that coincides with the appearance of vortex) change in the FDF is observed.

3.3 Effect of Addition of N_2 and Ar on Flame Response

In order to clarify the role of CO_2 addition in biogas flames, additional experiments were carried out, whereby two other diluents, namely N_2 and Ar, were added to the reference flame. For this study, the flow conditions were determined so that the same theoretical adiabatic flame temperature of the 10% CO_2 addition case (2170K) was achieved. Educational combustion software, GASEQ- A Chemical Equilibrium Program, was employed to determine the adiabatic flame temperatures. The percentage addition of N_2 and Ar required to achieve the same adiabatic flame temperature as that of 10% CO_2 were determined to be 20 % and 30 % respectively. The results from test cases with same adiabatic flame temperatures i.e 10% CO_2, 20%N_2 and 30%Ar are presented in Figs. 9-12. For consistency, the results from the reference flame condition,referred as '0% Diluent', have also been included in all the figures.

Figure 9 presents the variation in normalised heat release

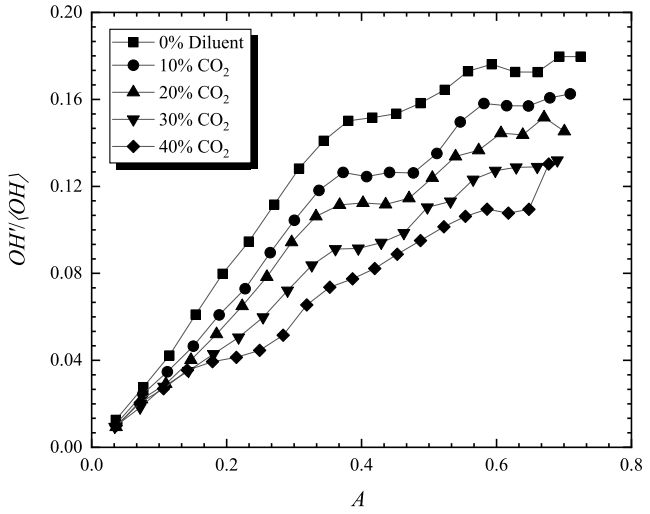

FIGURE 5. EFFECT OF CO_2 ADDITION ON THE DEPENDENCE OF NORMALISED HEAT RELEASE OSCILLATIONS ON THE NORMALISED FORCING AMPLITUDE A, AT FORCING FREQUENCY f=260 Hz, EVALUATED USING OH* CHEMILUMINESCENCE AND ACOUSTIC PRESSURE MEASUREMENTS.

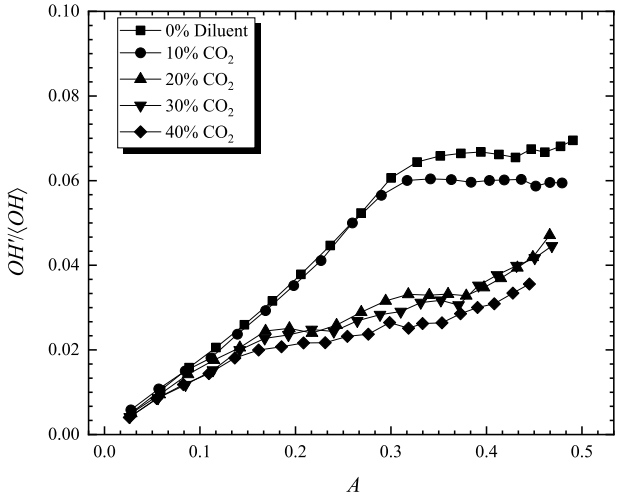

FIGURE 6. EFFECT OF CO_2 ADDITION ON THE DEPENDENCE OF NORMALISED HEAT RELEASE FLUCTUATION ON THE NORMALISED FORCING AMPLITUDE A, AT FORCING FREQUENCY f=345 Hz.

with respect to varying forcing amplitudes at f =260 Hz, for all cases with the same adiabatic flame temperature as that of the reference case. It can be noted that the trend for all the cases are similar, i.e, linear variation followed by saturation with respect to the amplitude increase. The magnitudes of variation for N_2 and Ar lie in between the 10% CO_2 addition and the reference

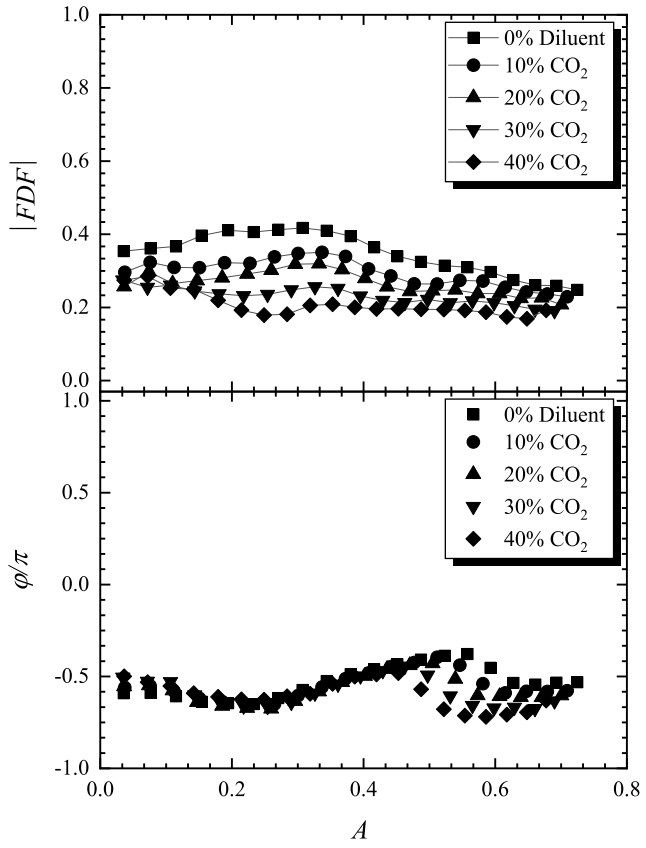

FIGURE 7. EFFECT OF CO_2 ADDITION ON THE MAGNITUDE AND THE NORMALISED PHASE OF THE FLAME DESCRIBING FUNCTION, FDF, AT FORCING FREQUENCY f=260 Hz.

case. Figure 11 presents the variation in normalised heat release with respect to varying forcing amplitude at f =345 Hz, for all cases with the same adiabatic flame temperature as that of the reference case. The flame response for both the cases, Ar and N_2 additions, had a lower magnitude of response compared to that of CO_2 addition and the reference case. The magnitude of heat release oscillation for the Ar dilution was higher than that of the (N2 dilution at both the forcing frequencies. It is clear from these results that the heat capacity between these three diluents could potentially be the biggest contributor to the observed behaviour. It has to be noted that, since nonlinear response is largely due to complex flame vortex interactions, the heat capacity difference is expected to influence the flame behaviour, as can be evidenced in these data sets of same adiabatic temperature conditions.

The variation in the magnitude of the flame describing function $|FDF|$ and the normalised phase for increasing amplitude of forcing at particular forcing frequency, exhibited similar trends for all the test cases presented (see Figs. 10 - 12). The amplitude dependency of the phase is largely a consequence of the kinematic flame response i.e., flame-vortex interactions. From the

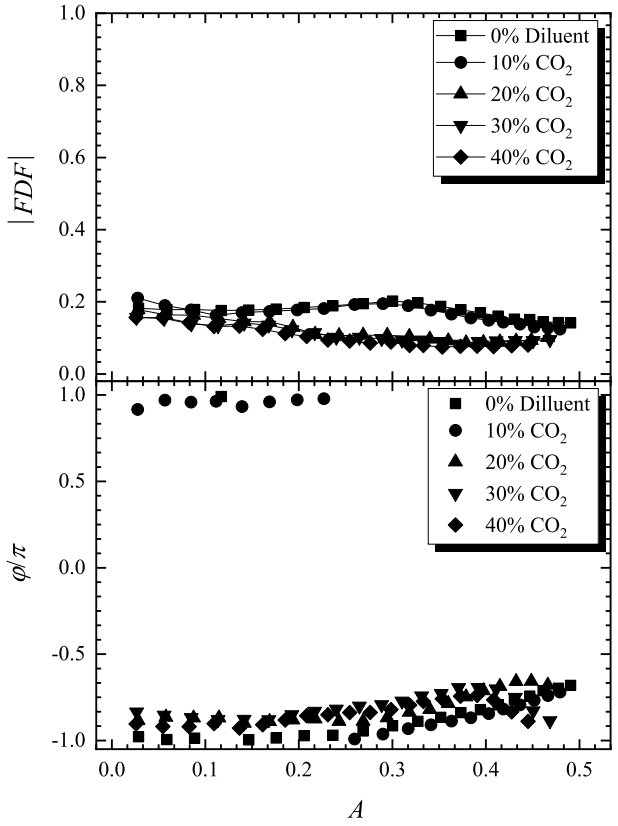

FIGURE 8. EFFECT OF CO_2 ADDITION ON THE MAGNITUDE AND THE NORMALISED PHASE OF THE FLAME DESCRIBING FUNCTION, FDF, AT FORCING FREQUENCY f=345 Hz.

amplitude dependency of the normalised phase presented here, we can conclude that for a fixed frequency, the mechanism of heat release response for all these dilution conditions is the same.

4 CONCLUSIONS

This paper describes an experimental investigation of non-linear flame response of simulated biogas flames. A laboratory scale combustor with a square optical enclosure was used for the study. Loudspeakers were used for acoustic excitation, while flame response was evaluated from simultaneous measurements of OH^* chemiluminescence and acoustic pressure measurements. Two-microphone method was used to determine the velocity perturbations. The focus of the work is to detail the effect of carbondioxide, CO_2, content on the acoustic response of the flames. The amplitude dependency of the flame dynamics was studied at different forcing frequencies, 260 Hz and 345 Hz. The addition of CO_2 to turbulent methane flames reduced the magnitude of heat release response at both the forcing frequencies, 260 Hz and 345 Hz. The results indicate that

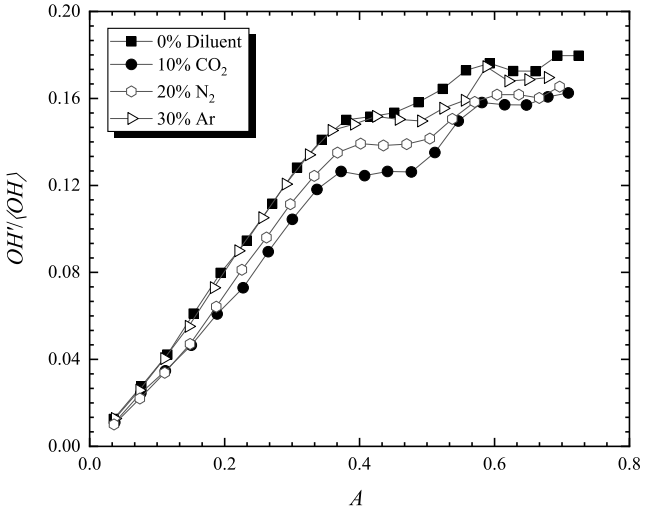

FIGURE 9. EFFECT OF DILUENT ADDITION ON HEAT RELEASE RESPONSE FOR FLAMES WITH SAME ADIABATIC FLAME TEMPERATURE (ESTIMATED FROM GASEQ), AT FORCING FREQUENCY f=260 Hz.

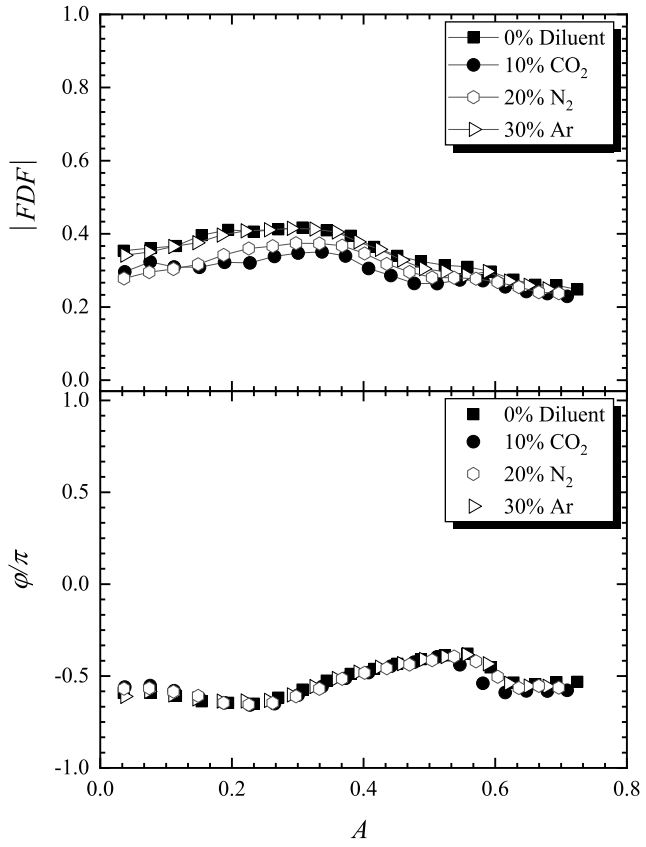

FIGURE 10. EFFECT OF DILUENT ADDITION ON FDF FOR FLAMES WITH SAME ADIABATIC FLAME TEMPERATURE AT FORCING FREQUENCY f=260 Hz.

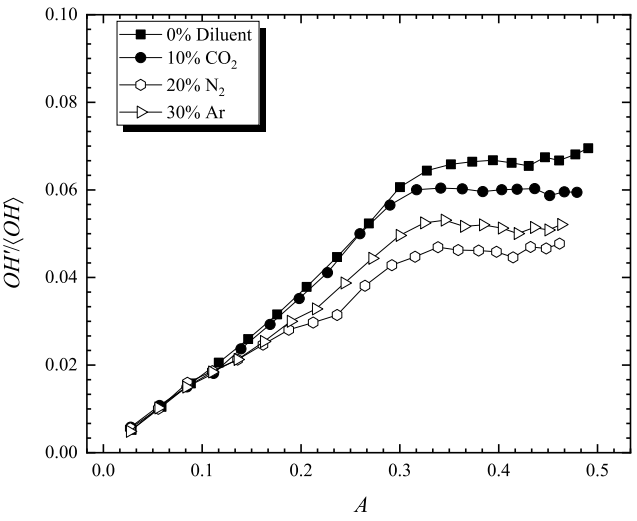

FIGURE 11. EFFECT OF DILUENT ADDITION ON HEAT RELEASE RESPONSE FOR FLAMES WITH SAME ADIABATIC FLAME TEMPERATURE AT FORCING FREQUENCY f=345 Hz

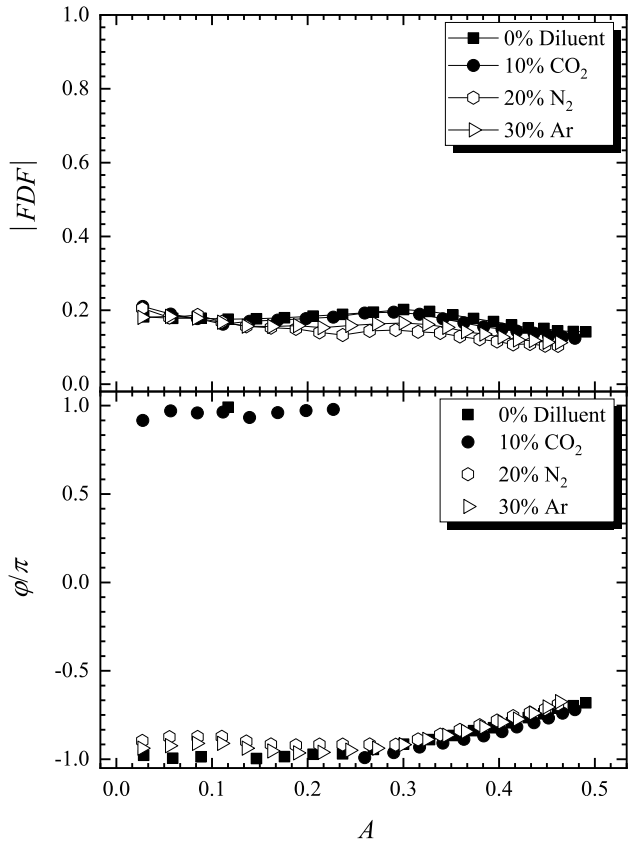

FIGURE 12. EFFECT OF DILUENT ADDITION ON *FDF* FOR FLAMES WITH SAME ADIABATIC FLAME TEMPERATURE AT FORCING FREQUENCY f=345 Hz.

the mechanisms of heat release variation and that of saturation could be considered to be the same for all flames studied. However, the observed differences in magnitudes of flame response for different diluents, CO_2, N_2 and Ar, could be attributed to differences in physical properties of the gases, such as thermal capacity. It is envisaged that the results obtained from this work will inform combustor design for utilisation of multi-component low calorific value fuels, and provide data for thermo-acoustic modellers. Future work will focus on detailed flame imaging and flame-flow interactions (that is, interactions between the side/central recirculation zones and the shear layers) to better understand the underpinning mechanisms related to the observed trends in nonlinear flame response.

ACKNOWLEDGMENT

The authors would like to acknowledge EPSRC (EP/P003036/1) for their financial support towards this work. Oluwaseun Ajetunmobi wishes to acknowledge Petroleum Technology Development Fund (PTDF) Nigeria for providing funding for her PhD study.

REFERENCES

[1] Stern, J. P., 2017. *The Future of Gas in Decarbonising European Energy Markets: the need for a new approach*. Oxford Institute for Energy Studies.

[2] Chen, H., He, J., and Zhong, X., 2018. "Engine combustion and emission fuelled with natural gas: A review". *Journal of the Energy Institute*.

[3] Qian, Y., Sun, S., Ju, D., Shan, X., and Lu, X., 2017. "Review of the state-of-the-art of biogas combustion mechanisms and applications in internal combustion engines". *Renewable and Sustainable Energy Reviews,* ***69***, pp. 50–58.

[4] Lieuwen, T., 2003. "Modeling premixed combustion-acoustic wave interaction: A review". *Journal of Propulsion and Power,* ***19***(5), pp. 765–781.

[5] Candel, S., 2002. "Combustion dynamics and control: Progress and challenges". *Proceedings of the Combustion Institute,* ***29***, pp. 1–28.

[6] Dowling, A. P., 2000. "The 1999 Lanchester lecture- Vortices, sound and flame -damaging combination". *Aeronautical Journal,* ***104***(1033), March, pp. 105–116.

[7] Runyon, J., 2017. "Gas turbine fuel flexibility: pressurized swirl flame stability, thermoacoustics, and emissions". PhD thesis, Cardiff University.

[8] Gökalp, I., and Lebas, E., 2004. "Alternative fuels for industrial gas turbines (aftur)". *Applied Thermal Engineering,* ***24***(11-12), pp. 1655–1663.

[9] Lieuwen, T., McDonell, V., Petersen, E., and Santavicca, D., 2008. "Fuel flexibility influences on premixed combus-

tor blowout, flashback, autoignition, and stability". *Journal of engineering for gas turbines and power,* ***130***(1), p. 011506.

[10] Dowlut, A. I., Hussain, T., Balachandran, R., and Swaminathan, N., 2012. "Experimental investigation of dynamic response of acoustically forced turbulent premixed ch 4/co 2/air flames". In 19th International Congress on Sound and Vibration 2012, ICSV 2012, Vol. 1, pp. 498–505.

[11] Ju, Y., Masuya, G., and Ronney, P. D., 1998. "Effects of radiative emission and absorption on the propagation and extinction of premixed gas flames". *Symposium (International) on Combustion,* ***27***(2), pp. 2619 – 2626.

[12] Liu, F., Guo, H., Smallwood, G. J., and Gülder, Ö. L., 2001. "The chemical effects of carbon dioxide as an additive in an ethylene diffusion flame: implications for soot and nox formation". *Combustion and Flame,* ***125***(1-2), pp. 778–787.

[13] Greco, A., Mira, D., and Jiang, X., 2017. "Effects of fuel composition on biogas combustion in premixed laminar flames". *Energy Procedia,* ***105***, pp. 1058–1062.

[14] Mazas, A., Lacoste, D., and Schuller, T., 2010. "Experimental and numerical investigation on the laminar flame speed of ch4/o2 mixtures diluted with co2 and h2o". In ASME Turbo Expo 2010: Power for Land, Sea, and Air, American Society of Mechanical Engineers, pp. 411–421.

[15] Shy, S., Yang, S., Lin, W., and Su, R., 2005. "Turbulent burning velocities of premixed ch4/diluent/air flames in intense isotropic turbulence with consideration of radiation losses". *Combustion and Flame,* ***143***(1-2), pp. 106–118.

[16] Balachandran, R., Ayoola, B. O., Kaminski, C. F., Dowling, A. P., and Mastorakos, E., 2005. "Experimental investigation of the non-linear response of turbulent premixed flames to imposed inlet velocity oscillations". *Combustion and Flame,* ***143***(1-2), October, pp. 37–55.

[17] Lee, J. G., and Santavicca, D. A., 2003. "Experimental diagnostics for the study of combustion instabilities in lean premixed combustors". *Journal of Propulsion and Power,* ***19***(5), pp. 735–750.

[18] Quintino, F., Trindade, T., and Fernandes, E., 2018. "Biogas combustion: Chemiluminescence fingerprint". *Fuel,* ***231***, pp. 328–340.

[19] Seybert, A. F., and Ross, D. F., 1977. "Experimental determination of acoustic properties using a two-microphone random-excitation technique". *the Journal of the Acoustical Society of America,* ***61***(5), pp. 1362–1370.

[20] Palies, P., Durox, D., Schuller, T., and Candel, S., 2010. "The combined dynamics of swirler and turbulent premixed swirling flames". *Combustion and Flame,* ***157***(9), pp. 1698–1717.

[21] Hussain, T., and Balachandran, R., 2011. "Investigation of the effect of fuel stratification on response of turbulent premixed flames to acoustic excitation". In 18th International Congress on Sound and Vibration 2011, ICSV 2011, Vol. 1, pp. 529–536.